ORGANOMETALLICS

pubs.acs.org/Organometallics Article

Catalytic Hydrogenation of Alkenes and Alkynes by a Cobalt Pincer Complex: Evidence of Roles for Both Co(I) and Co(II)

Hussah Alawisi, Hadi D. Arman, and Zachary J. Tonzetich*

Cite This: https://dx.doi.org/10.1021/acs.organomet.1c00053 Read Online

ACCESS | Metrics & More | Article Recommendations | Supporting Information

ABSTRACT: The Co(I) complex, [Co(N_2)(^{Cy}PNP)] (^{Cy}PNP = anion of 2,5-bis-(dicyclohexylphosphinomethyl)pyrrole), is active toward the catalytic hydrogenation of terminal alkenes and the semi-hydrogenation of internal alkynes under 2 bar of H_2 (g) at room temperature. The products of alkyne semi-hydrogenation are a mixture of *E*- and *Z*-alkenes. By contrast, use of the related cobalt(I) precatalyst, [Co(PMe_3)-(^{Cy}PNP)], results in formation of exclusively *Z*-alkenes. A semi-stable Co(II) species, [CoH(^{Cy}PNP)], can also be generated by treatment of degassed solutions of [Co(N_2)(^{Cy}PNP)] with H_2. The Co^{II}-hydride displays activity toward both alkene hydrogenation and isomerization, but its instability hampers implementation as a catalyst. Several species relevant to potential catalytic intermediates have been isolated and detected in solution. These compounds include alkene and alkyne adducts of Co(I) as well as a Co(III) dihydride species. Catalytic results with the compounds examined are most consistent with a process involving shuttling between Co(I) and Co(III) states. However, generation of small quantities of Co(II) during catalytic turnover appears to be responsible for the isomerization observed for alkyne semi-hydrogenation. The interplay of cobalt oxidation states within the same catalyst system is discussed in the context of mechanistic scenarios for catalytic hydrogenation.

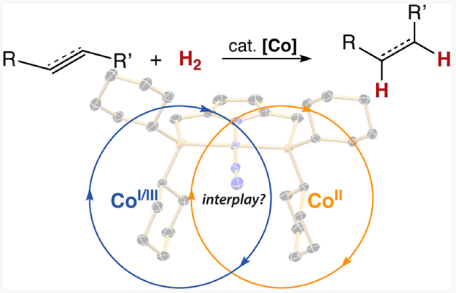

INTRODUCTION

The catalytic hydrogenation of unsaturated compounds encompasses one of the foremost applications of organometallic chemistry to organic synthesis. For decades, precious metals have been employed for the hydrogenation reaction in both heterogeneous and homogeneous catalyst systems. Despite the efficacy and selectivity of these catalysts across a variety of substrates, recent work, particularly in the area of homogeneous catalysis, has seen a shift in focus to more earth-abundant transition metal systems. Several first-row transition metals have shown great promise as homogeneous hydrogenation catalysts with activities rivaling their precious metal counterparts in several instances.[1−9] The ligand frameworks used to support these systems vary, but pincers have emerged as an especially effective class of ligands for the creation of well-defined catalysts.[10,11] Use of pincer ligands among the mid 3*d* metals (Mn, Fe, and Co) has permitted detailed investigations into the mechanisms of catalytic hydrogenations, revealing pathways unique from those of precious metal systems.[12−16]

In the area of cobalt chemistry, reports from several groups have described the catalytic hydrogenation activity of well-defined cobalt catalysts featuring pincer ligands.[17−31] These catalysts have been applied successfully for the hydrogenation of olefins and semi-hydrogenation of alkynes, with several systems displaying impressive stereoselectivities. Despite this success, no unified mechanistic picture has arisen comparable to the better understood features of H_2 activation and olefin insertion at play with heavier Group 9 metals. There are two primary mechanistic cycles proposed for hydrogenation of alkenes and alkynes by Co-based catalysts (Scheme 1). The key difference in these two mechanisms stems from the oxidation states of the cobalt centers and the nature of H_2 activation. In the first mechanism (**A**), a Co(I) species activates molecular hydrogen by oxidation addition to give a Co(III) dihydride, often via a dihydrogen complex.[23,32] Olefin or alkyne then undergoes migratory insertion into the Co−H bond to generate an intermediate cobalt-hydrido-hydrocarbyl species. Facile reductive elimination from this Co(III) species affords the reduced product and closes the cycle. In the second mechanism (**B**), a Co(II)-hydride species is operative, which is also capable of undergoing migratory insertion with olefin or alkyne to form the corresponding hydrocarbyl compound.[33] Hydrogenolysis of the Co(II)-hydrocarbyl, most likely through a sigma-bond metathesis process, produces the reduced product and regenerates the active hydride. Both of these mechanisms have been put forward for different systems, demonstrating the important role of the supporting ligand in dictating the catalytic chemistry.

Received: January 29, 2021

https://dx.doi.org/10.1021/acs.organomet.1c00053
Organometallics XXXX, XXX, XXX−XXX

Scheme 1. Canonical Mechanisms for Co-Catalyzed Alkene/Alkyne Hydrogenation

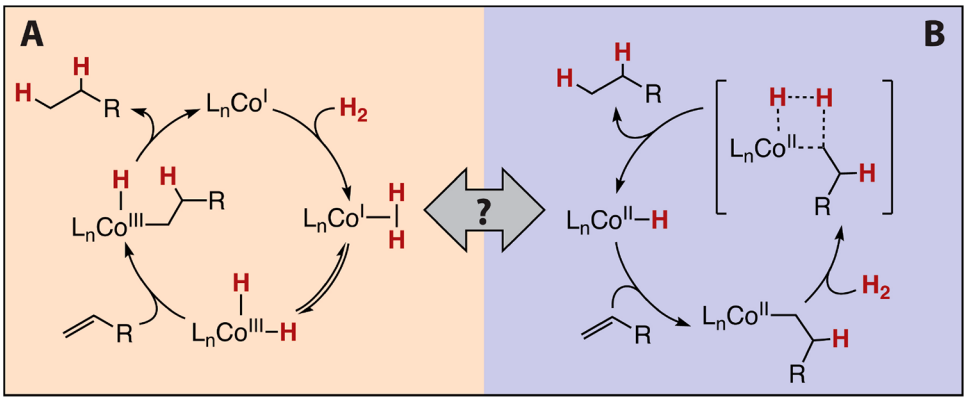

Our laboratory has been investigating the reactivity of cobalt complexes supported by a pyrrole-based PNP ligand, ^{R}PNP (^{R}PNP = anion of bis(dialkylphosphinomethyl)pyrrole).[34] These compounds have shown efficacy in several reductive bond activation reactions including C-X oxidative addition and aldehyde decarbonylation.[35] To further establish the potential of this system in reductive transformations, we turned our attention to the hydrogenation of alkenes and alkynes. In this contribution, we describe the catalytic behavior of the ^{Cy}PNPCo platform toward hydrogenation and the unexpected role that both Co(I) and Co(II) can play in the catalytic cycle. This work thereby establishes a link between the two most prevalent mechanisms put forward for cobalt hydrogenation catalysts.

RESULTS AND DISCUSSION

Stoichiometric Reactivity. We began our investigations by examining the reactivity of several well-defined cobalt(II) and cobalt(I) species with molecular hydrogen to simulate likely steps in catalytic cycles involving both oxidation states. Exposure of benzene-d_6 solutions of the alkyl Co(II) complexes, [CoR(^{Cy}PNP)] (R = Me, Ph), to 1−5 bar of H_2 was found to result in no discernible reactivity over the course of several hours at ambient temperature as judged by NMR spectroscopy. In contrast, similar treatment of the trimethylsilylmethyl analogue, [Co(CH_2SiMe_3)(^{Cy}PNP)] (**1**, Figure 1), with H_2 proceeded slowly to generate Me_4Si and a small amount of a new paramagnetic species that we assign as the putative hydride complex, [CoH(^{Cy}PNP)] (**2**, eq 1).

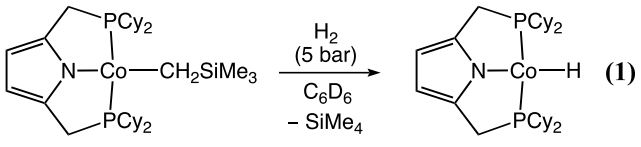

(1)

Attempts to generate **2** in larger quantities by treatment of [CoX(^{Cy}PNP)] (X = Cl, Br) with hydride sources were unsuccessful, resulting primarily in recovery of the cobalt(I) species, [Co(N_2)(^{Cy}PNP)] (**3**) (see Supporting Information). We encountered similar issues in prior work with Co(II) complexes of the bulkier ^{tBu}PNP ligand, ascribing the propensity for reduction, in part, to the stable nature of the cobalt(I) dinitrogen complex.[36] We now find that solutions of **2** can be generated from either **1** or [CoX(^{Cy}PNP)], but only in the absence of N_2. Accordingly, treatment of degassed

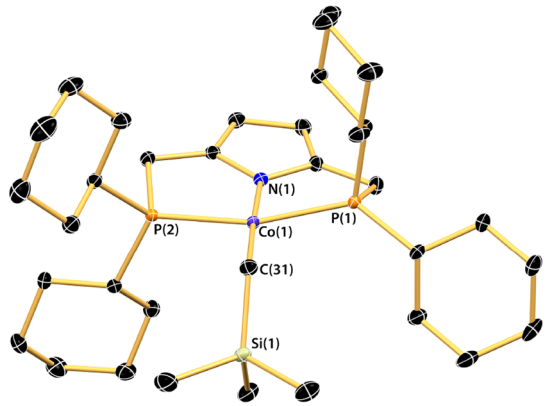

Figure 1. Thermal ellipsoid plot (50%) of the solid-state structure of **1**. Hydrogen atoms are omitted for clarity. Selected bond lengths (Å) and angles (deg): Co(1)−C(31) = 1.9998(14); Co(1)−N(1) = 1.9006(12); Co(1)−P_{avg} = 2.212(4); P(1)−Co(1)−P(2) = 162.477(16); N(1)−Co(1)−C(1) = 177.88(6); Co(1)−C(31)−Si(1) = 116.99(8).

solutions of [CoX(^{Cy}PNP)] with $KHBEt_3$ generated **2** as the sole product as judged by ^{1}H NMR spectroscopy (eq 2).

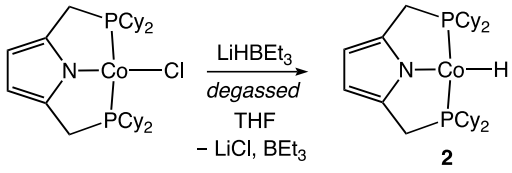

(2)

Likewise, addition of H_2 to degassed solutions of **1** similarly gave rise to **2**. Compound **2** remains stable in solution if excluded from N_2, but rapidly reverts to **3** when a nitrogen atmosphere is introduced. The paramagnetic ^{1}H NMR spectrum of **2** resembles that of other square-planar cobalt(II) complexes of the ^{Cy}PNP ligand, suggesting a similar coordination geometry and $S = {}^1/_2$ spin state (see Supporting Information).[37]

In similar fashion to the results with divalent hydrocarbyl species, treatment of the cobalt(I)-N_2 adduct, **3**, with 1−5 bar of H_2 resulted in no discernible reactivity when conducted in the presence of N_2. However, when H_2 was introduced to degassed solutions of **3**, a mixture of **2** and **3** was produced as judged by NMR spectroscopy (Scheme 2). Thus, H_2 appears to provide a conduit between cobalt(I) and cobalt(II) under appropriate conditions. At present, we can only speculate on

https://dx.doi.org/10.1021/acs.organomet.1c00053
Organometallics XXXX, XXX, XXX−XXX

Scheme 2. Reactivity of 3 with Hydrogen

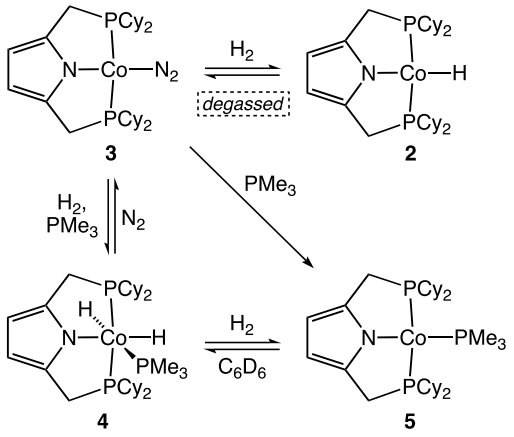

the mechanism underlying formation of **2** from **3** and H_2, but we favor a process involving reversible generation of a Co(I)-H_2 adduct in the absence of N_2. Subsequent oxidative addition to give a Co(III) dihydride, followed by either loss of H· or comproportionation with unreacted **3**, would then afford **2**. Reversible oxidative addition of H_2 to cobalt(I) has been observed in related pincer systems reported by the groups of Chirik and Fout.[23,38] In these cases, however, cobalt(III) dihydride species can be identified as the products of H_2 addition. Moreover, stabilization of the dihydride species is found to require coordination of an additional ligand. We therefore examined the reaction of compound **3** with H_2 in the presence of PMe_3 in order to determine if H_2 activation occurs in similar fashion to that observed with degassed solutions of **3**. Surprisingly, the ^{1}H NMR spectrum of the resulting reaction mixture demonstrated the formation of a new diamagnetic cobalt species with a broad resonance apparent in the hydride region near −18 ppm. In addition, the ^{31}P NMR spectrum displayed two new peaks at 88.5 and 3.5 ppm. These spectroscopic features are consistent with formation of a new diamagnetic cobalt(III) complex (**4**, Scheme 2). ^{1}H NMR spectra acquired at 257 K in toluene-d_8 further supported the composition of **4**, showing two broadened hydride resonances at −14.1 and −21.6 ppm. Solutions of compound **4** are not stable in the absence of H_2 and quickly revert to the cobalt(I)-PMe_3 adduct, [Co(PMe_3)(^{Cy}PNP)] (**5**). Likewise, attempts to isolate **4** resulted only in recovery of **5**. Compound **5** could be prepared directly by treatment of **3** with PMe_3 (Scheme 2) The solid-state structure of **5** can be found in the Supporting Information and resembles that of **3**. In agreement with the three-component reaction described above, direct treatment of **5** with H_2 also generated dihydride **4** as judged by ^{1}H and ^{31}P NMR spectroscopy.

The reactivity of **3** and **5** with molecular hydrogen establishes the viability of both cobalt(II) and cobalt(III) oxidation states as products of H_2 activation by cobalt(I). It remains possible, however, that the direct reaction of H_2 with **3** may be less favorable then association of substrates such as alkenes and alkynes in the context of hydrogenation chemistry. We therefore turned our attention to the reactivity of **3** with unsaturated hydrocarbons, reasoning that adduct formation with either substrate may represent a resting state in the catalytic cycle and obviate the need for direct H_2 reaction with **3**. Moreover, as observed with **5**, coordination of additional ligands to **3** can direct oxidative addition chemistry in favor of Co(III) dihydride species. Addition of diphenylacetylene to **3** or **5** produced a new diamagnetic species as judged by NMR spectroscopy (see Supporting Information). Both ^{1}H and ^{31}P NMR spectra are indicative of C_{2v} symmetry, consistent with symmetrical coordination of the alkyne to the cobalt center (**6**, Scheme 3). Despite the apparent stability of compound **6**, we have been unable to crystallize the molecule in satisfactory fashion for further analysis.

Scheme 3. Reactivity of 3 with Alkynes and Alkenes

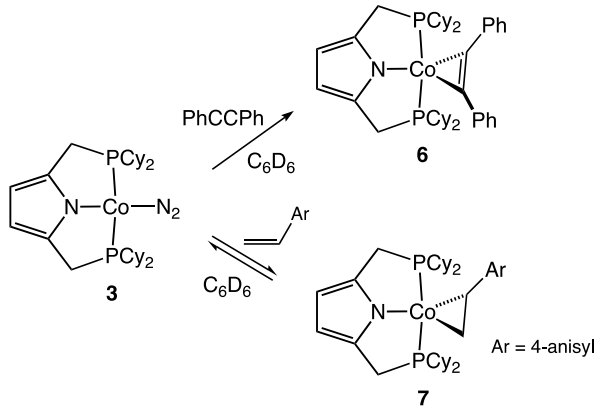

Similar reaction of **3** with styrene derivatives gave rise to a mixture of the unreacted starting material and a new diamagnetic compound displaying NMR resonances indicating loss of C_{2v} symmetry. In the case of 4-vinylanisole, the ^{1}H NMR spectrum exhibits broadened resonances for both the vinylic H atoms as well as the methylene arms of the ligand. In addition, the ^{31}P NMR spectrum shows an AB pattern for the two phosphorus nuclei (see Supporting Information). These spectroscopic features are all consistent with a complex featuring a π-coordinated olefin in which there is some degree of fluxional motion (**7**, Scheme 3). Isolation of compound **7** proved difficult owing to equilibrium dissociation of the olefin, but crystallization from solutions of excess 4-vinylansiole permitted isolation of a few single crystals suitable for X-ray diffraction. The solid-state structure of **7** is displayed in Figure 2. The molecule exhibits the expected face-on binding of the olefin to the cobalt center with an overall coordination geometry approximating square-planar. The olefin is bound vertically with respect to the square plane of the molecule within the cleft created by the flanking phosphine substituents. The Co−C contacts of 2.022(2) and 2.067(2) Å are inequivalent, most likely as a result of stronger steric interactions between the anisyl group and the cyclohexyl rings.

The ability of π systems to coordinate to the ^{Cy}PNPCo^I fragment next prompted us to examine the reactivity of the alkyne adduct **6** with molecular hydrogen. Given our observations with **3**, we anticipated that the alkyne ligand might activate the cobalt center toward H_2 oxidative addition. Gratifyingly, addition of 1 bar of H_2 (substoichiometric) to a benzene-d_6 solution of compound **6** was observed to give rise to a mixture of unreacted **6**, compound **3**, and *cis*-stilbene as judged by ^{1}H NMR spectroscopy. This result demonstrates that compound **6**, and by extension compound **3**, are viable candidates for alkyne hydrogenation precatalysts.

As a final aspect of the stoichiometric chemistry of **3**, we sought to probe its reactivity with terminal alkynes. As substrates, terminal alkynes have proved challenging in

https://dx.doi.org/10.1021/acs.organomet.1c00053
Organometallics XXXX, XXX, XXX−XXX

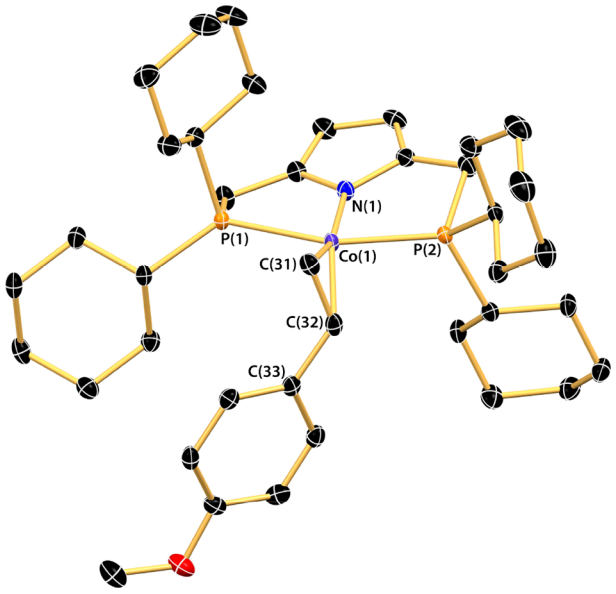

Figure 2. Thermal ellipsoid (50%) drawing of the solid-state structure of compound **7**. Hydrogen atoms have been omitted for clarity. Selected bond distances (Å) and angles (deg): Co(1)−C(31) = 2.022(2); Co(1)−C(32) = 2.0672(19); Co(1)−N(1) = 1.9068(16); Co(1)−P_{avg} = 2.2282(5); C(31)−C(32) = 1.404(3); P(1)−Co(1)−P(2) = 161.80(2); N(1)−Co(1)−CC_{centr} = 177.28(8).

hydrogenation protocols featuring cobalt catalysts.[25] This incompatibility is not unexpected given the enhanced reactivity of the C_{sp}−H bond, which can engage in orthogonal chemistry, limiting catalytic turnover. In the case of **3**, treatment with phenylacetylene led to immediate formation of the Co(II) acetylide complex, **8** (eq 3). Compound **8** displays a

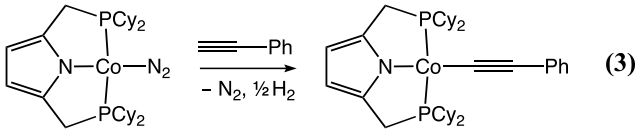

3 **8** **(3)**

paramagnetic ^{1}H NMR spectrum akin to that of **1** and **2**, consistent with a low-spin Co(II) center. The solid-state structure of **8** is displayed in Figure 3 and is consistent with other square-planar Co(II) hydrocarbyl species such as **1**.

Formation of **8** mostly likely occurs via initial oxidative addition of the alkyne C−H bond to **3** in similar fashion to what we observed previously for carboxylic acids.[35] In order to capture the possible Co(III) intermediate responsible for this chemistry, we examined the same reaction in the presence of PMe_3. Much like the case for **4**, we anticipated that phosphine ligation would stabilize the Co(III) species. Accordingly, addition of phenylacetylene to **5** produced a new diamagnetic spectrum displaying a doublet of triplets resonance for the Co-H centered at −11.64 ppm (see Supporting Information). The values for the $^2J_{HP}$ coupling constants of 55 and 135 Hz indicate a *cis* arrangement of the two P atoms of the pincer and a *trans* disposition of the PMe_3 ligand with respect to the hydride. Although stable in solution for several hours, we have been unable to isolate this hydride species. Nonetheless, observation of this species supports a reaction pathway for terminal alkynes featuring C-H oxidative addition. In the absence of PMe_3, the corresponding alkynyl-hydride is unstable and rapidly leads to formation of compound **8**.

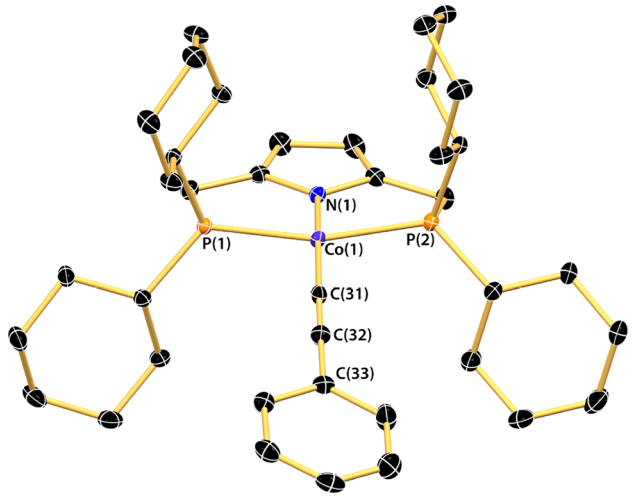

Figure 3. Thermal ellipsoid (50%) drawing of the solid-state structure of **8**. Hydrogen atoms have been omitted for clarity. Selected bond distances (Å) and angles (deg): Co(1)−C(31) = 1.8693(19); Co(1)−N(1) = 1.8699(15); Co(1)−P_{avg} = 2.1987(5); C(31)−C(32) = 1.226(3); P(1)−Co(1)−P(1) = 164.09(2); N(1)−Co(1)−C(31) = 171.99(7); C(31)−C(32)−C(33) = 177.7(2).

Catalytic Reactions with Alkenes. In an initial set of experiments, we examined the catalytic activity of compounds **1** and **3** toward the hydrogenation of styrene in benzene-d_6. We also tested the bulkier variant, [Co(N_2)(^{tBu}PNP)], to determine if enhanced steric encumbrance about the metal center plays a role in catalytic efficacy. At room temperature under 2 bar of H_2, both complexes **1** and **3** promoted the catalytic hydrogenation of styrene to afford ethylbenzene at a loading of 2 mol % as judged by NMR spectroscopy. With **3** as a catalyst, the reaction proceeded to full conversion over 2 h; however, the use of **1** resulted in only 25% yield of ethylbenzene. This lower yield observed for **1** likely reflects the difficulty in forming **2** and its attendant instability, which is the presumed active species (*vide infra*). In contrast to the results with **1** and **3**, the bulkier [Co(N_2)(^{tBu}PNP)] complex did not promote hydrogenation of styrene under the conditions examined.

Given the preliminary results with styrene, we turned our attention to compound **3** as a precatalyst for olefin hydrogenation. Using *p*-chlorostyrene as a test substrate, we investigated the role of solvent and catalyst loading. Reactions performed in the absence of solvent led to low conversion, likely due to strong coordination of the alkene to the catalyst (*vide supra* compound **7**). Furthermore, replacing benzene with THF as solvent also afforded lower conversion, indicating that noncoordinating solvents are most suitable. In terms of catalyst loading, increasing the amount of precatalyst employed from 0.5 to 2 mol % led to a corresponding climb in conversion, consistent with some amount of catalyst deactivation during turnover.

We next looked at a series of different olefinic substrates. In all cases, formation of the corresponding alkane was observed, although some classes of substrates required longer reactions times (Table 1). Electronic effects, as seen with *para* substituted styrene derivatives, demonstrated that electron-withdrawing groups (EWG) provided lower yields compared with the parent styrene and that containing a methoxy group (Table 1, entries 1−3). We attribute this result to inhibition by an alkene adduct, which should prove more stable for alkenes

https://dx.doi.org/10.1021/acs.organomet.1c00053
Organometallics XXXX, XXX, XXX−XXX

Table 1. Alkene Hydrogenation by Compound 3[a]

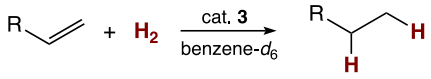

Entry	Alkene	Time	Yield
1	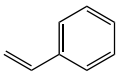	60 min	95%
2	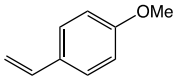	30 min	94%
3	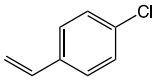	30 min	86%
4		22 h	n.r.
5		22 h	n.r.
6	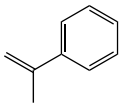	22 h	n.r.
7	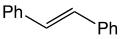	22 h	n.r.
8	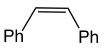	2 h	n.r.[b]
9	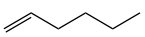	60 min	61%
10	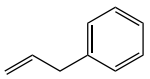	90 min	94%

[a]All reactions performed with 2 mol % of **3** under 2 bar of H_2 in 1 mL of benzene-d_6; yields were determined by ^{1}H NMR spectroscopy with respect to an internal standard of 1,3,5-trimethylbenzene. [b]‡ *trans*-Stilbene detected in 41% yield.

bearing EWG substituents. In contrast to styrene derivatives, our system failed to hydrogenate internal alkenes, as shown in entries 4−7 of Table 1. Notably, attempted hydrogenation of *cis*-stilbene did not give the corresponding alkane, but instead led to formation of the isomerization product, *trans*-stilbene, in 41% yield (Table 1, entry 8).

Unlike the results from catalytic trials with **3**, stoichiometric reactions of both cyclohexene and *cis*-stilbene with H_2 in the presence of *in situ*-generated **2** resulted in formation of the corresponding alkanes. These results demonstrate that **2** has the capacity to serve as an efficient catalyst for alkene hydrogenation but that catalyst deactivation, most likely via formation of **3**, renders the hydride inactive after a few turnovers.

Catalytic Reactions with Alkynes. The results observed with internal alkenes demonstrate that **3** is incapable of hydrogenating such substrates under the conditions employed. We therefore reasoned that the catalyst system would be suitable for the semi-hydrogenation of internal alkynes. Indeed, **3** proved effective for such reactions. In a representative experiment, hydrogenation of diphenylacetylene was found to proceed to full conversion over 4 h when using 2 mol % of **3** as a catalyst in benzene-d_6 under 2 bar of H_2. The products of hydrogenation were found to be a mixture of *E*- and *Z*-stilbene isomers (ca. 9:1, respectively) in an overall yield of 90%. Surprisingly, addition of 1 equiv of PMe_3 with respect to **3** under identical conditions resulted in selective formation of *Z*-stilbene in 54% yield with no *E*-stilbene detectable by NMR spectroscopy. Similar results were obtained by using isolated **5** as a precatalyst.

The presence of PMe_3 in these reactions likely serves to deactivate the cobalt catalyst toward isomerization of the initially produced *Z*-alkene. We believe this inhibition occurs by preventing formation of **2** during catalytic turnover. As discussed above, the addition of PMe_3 to the reaction of **3** with H_2 results in cleaner formation of the cobalt(III) dihydride species **4**. Thus, by diverting the chemistry exclusively to the Co(I)/Co(III) pathway, the presence of PMe_3 is able to avoid formation of **2**, which is most likely responsible for isomerization (*vide infra*). The use of a *bona fide* Co(II) precatalyst, **1**, under the standard conditions, afforded only 25% yield of the *Z*-stilbene. We attribute this low yield and lack of isomerization to inefficient formation of **2** from **1** during catalytic turnover (cf. eq 1).

Next, we investigated the scope of alkyne hydrogenation by both **3** and **5**. In general, both complexes provided modest to good yields of the semi-hydrogenated products (Table 2). As with diphenylacetylene, **3** was found to produce a mixture of *E* and *Z* isomers in most instances, whereas **5** led to selective formation of the *Z*-alkene. These results are further consistent with the hypothesis that **2** can form in small quantities from **3** during catalytic turnover and mediate olefin isomerization.

Table 2. Alkyne Semi-hydrogenation by Compounds 3 and 5[a]

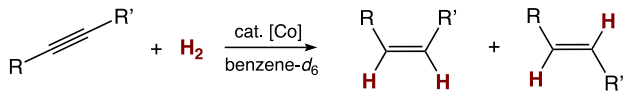

Entry	Alkyne	*E*:*Z* Ratio (Yield) **3**	**5**
1		> 98% *Z* (53%)	> 98% *Z* (49%)
2	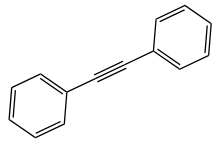	9:1 (90%)	> 98% *Z* (79%)
3	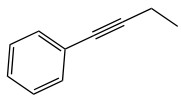	1:2 (48%)	> 98% *Z* (45%)
4	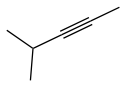	1:3 (47%)	> 98% *Z* (62%)
5	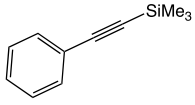	98:2 (98%)	> 98% *Z* (43%)
6	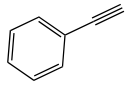	n.r.	n.r.

[a]All reactions performed with 2 mol % of **3** under 2 bar of H_2 in 1 mL of benzene-d_6 for 4 h; yields were determined by ^{1}H NMR spectroscopy with respect to an internal standard of 1,3,5-trimethylbenzene.

https://dx.doi.org/10.1021/acs.organomet.1c00053
Organometallics XXXX, XXX, XXX−XXX

Scheme 4. Proposed Mechanism for Alkyne Semi-hydrogenation by Compound 3

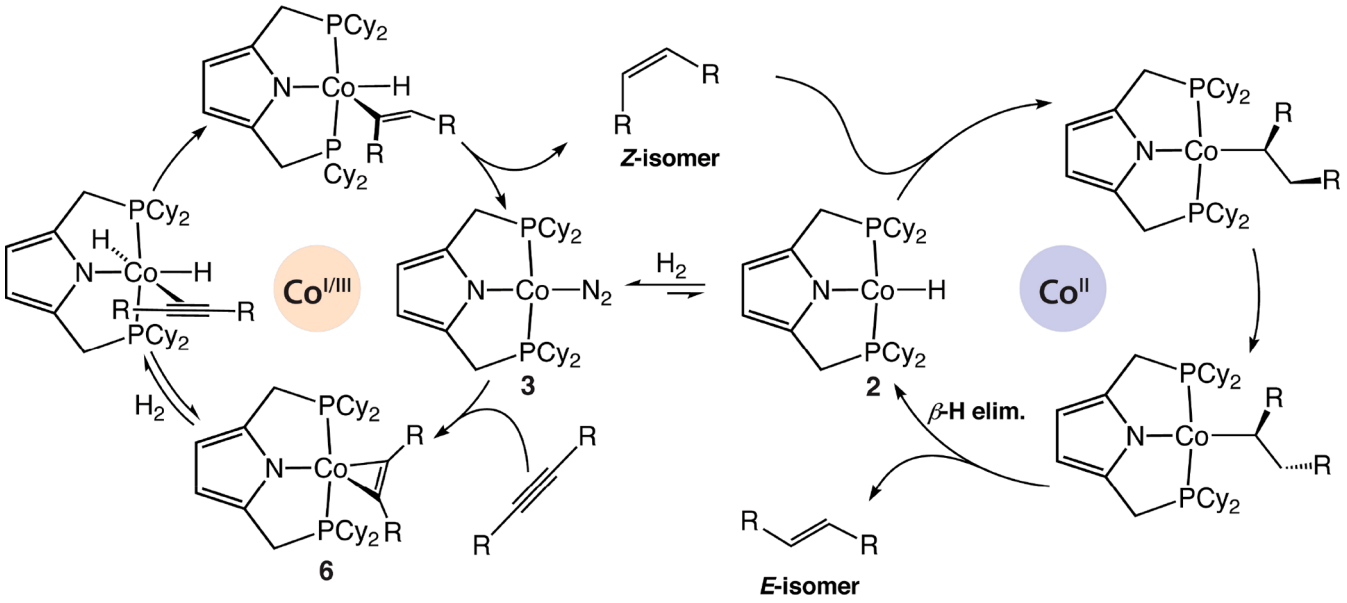

Moreover, dropping the catalyst loading to 1 mol % was found to lead to higher *Z*:*E* ratios in the case of diphenylacetylene. Such a result is logical since reducing the catalyst loading further attenuates the ability of **2** to form from **3**, thereby decreasing the likelihood of isomerization. As a final substrate class, terminal alkynes were investigated in hydrogenation reactions with **3** but proved unsuccessful. We attribute this lack of productive reactivity to the facile activation of the C−H bond leading to formation of compounds such as **8**.

Alkene Isomerization. The differential quantities of *trans* olefin observed during alkyne semi-hydrogenation with precatalysts **3** and **5** implies that a species other than a Co(III)-hydride is responsible for isomerization. Furthermore, the isomerization event most likely occurs subsequent to hydrogenation of the alkyne as observed in several other systems.[24,39] To verify this possibility, we examined the hydrogenation of diphenylacetylene by **3** in the presence of 1 equiv of *cis*-stilbene. The reaction was found to proceed, but *trans*-stilbene was not detected until all the PhCCPh was consumed, as judged by NMR, confirming that isomerization takes place after hydrogenation. We also directly compared the isomerization activity of **3** and **5** under 2 bar of H_2 employing *cis*-stilbene. Compound **3** demonstrated good activity, producing a mixture of stilbenes within 5 min. By contrast, **5** required 12 h to produce detectable quantities of *trans*-stilbene.

On the basis of these results, a logical proposal for the observed isomerization encountered during alkyne hydrogenation implicates compound **2**. As discussed above, **2** is observed to form from **3** and H_2, especially in the absence of additional ligands. In the presence of alkyne, compound **6** is formed from either precatalyst **3** or **5** and hinders formation of small quantities of **2**. As alkyne is hydrogenated to alkene, compound **3** becomes the major cobalt containing species and is subject to reaction with H_2 to form **2**. With **5** as a precatalyst, however, the presence of PMe_3 further prevents formation of **2** even when all the alkyne is consumed. In those reactions where the concentration of **2** can accumulate (i.e., those employing **3**), isomerization of the new alkene can take place.

As a final test of our proposed mechanism, we investigated if *in situ* generated **2** was in fact active toward alkene isomerization. Gratifyingly, treatment of **2** with *cis*-stilbene caused immediate formation of the *trans* isomer in the absence of added H_2. We therefore favor a scenario for cobalt-catalyzed hydrogenation as shown in Scheme 4. The $Co^{I/III}$ couple appears to be responsible for the hydrogenation of alkynes and terminal alkenes as observed in other systems, but isomerization and/or hydrogenation of substituted alkenes must proceed through Co^{II}. Suppression of cobalt(II) species by addition of PMe_3 (precatalyst **5**) results in more selective semi-hydrogenation of internal alkynes.

CONCLUSIONS

In this contribution, we have demonstrated the catalytic hydrogenation activity of a well-defined cobalt system employing a PNP pincer ligand. The cobalt catalyst, typified by the N_2-adduct **3**, was active for the hydrogenation of terminal alkenes as well as the semi-hydrogenation of internal alkynes through a mechanism most consistent with a $Co^{I/III}$ cycle (Figure 1, panel A). Use of a related cobalt(II)-hydride species, **2**, permitted hydrogenation of internal alkenes, but the instability and difficulty in generating this species precluded its use as catalyst. In the case of alkyne semi-hydrogenation, we could influence the formation of *E*- or *Z*-alkenes through judicious choice of precatalyst. The propensity for isomerization was found to correlate with the formation of compound **2**, which is suppressed in the case of added phosphine (Scheme 4). As a whole, these results demonstrate that interplay between Co(I) and Co(II), mediated by H_2, can play an important role during catalytic hydrogenation. Such behavior is unique to earth-abundant transition metal systems owing to their propensity to engage in one-electron chemistry. The generality of this phenomenon is likely to extend beyond the present cobalt system to other catalysts based on 3*d* metals.

EXPERIMENTAL SECTION

General Comments. All manipulations were performed under an atmosphere of purified nitrogen gas using a Vacuum Atmospheres glovebox. Tetrahydrofuran, diethyl ether, pentane, and toluene were

https://dx.doi.org/10.1021/acs.organomet.1c00053
Organometallics XXXX, XXX, XXX−XXX

purified by sparging with argon and passage through two columns packed with 4 Å molecular sieves and/or activated alumina (THF). ^{1}H NMR spectra were recorded on a Bruker spectrometer operating at 500 MHz (^{1}H) in benzene-d_6 unless otherwise noted and referenced to the residual protium resonance of the solvent (δ 7.16 ppm). ^{31}P NMR spectra were recorded at 202 MHz and referenced automatically using the ^{2}H lock frequency. Elemental analyses were performed by the CENTC facility at the University of Rochester. In each case, recrystallized material was used for combustion analysis.

Materials. [Co(N$_2$)(^{Cy}PNP)] (**3**), [CoX(^{Cy}PNP)] (X = Cl, Br), and [CoN$_2$(^{tBu}PNP)] were prepared according to published procedures.[35,36] Hydrogen gas was obtained from Airgas and delivered to NMR samples or reaction mixtures via a needle/septum. For larger pressures of H$_2$ (2−5 bar), a medium-pressure NMR tube was employed with a direct connection to the gas regulator. All other reagents were purchased from commercial suppliers and used as received.

Crystallography. Crystals suitable for X-ray diffraction were mounted, using Paratone oil, onto a nylon loop. All data were collected at 98(2) K using a Rigaku AFC12/Saturn 724 CCD fitted with Mo Kα radiation (λ = 0.71075 Å). Low-temperature data collection was accomplished with a nitrogen cold stream maintained by an X-Stream low-temperature apparatus. Data collection and unit cell refinement were performed using CrystalClear software.[40] Data processing and absorption correction, giving minimum and maximum transmission factors, were accomplished with CrysAlisPro[41] and SCALE3 ABSPACK,[42] respectively. The structure, using Olex2,[43] was solved with the ShelXT[44] structure solution program using direct methods and refined (on F^2) with the ShelXL refinement package using the full-matrix, least-squares techniques.[45] All nonhydrogen atoms were refined with anisotropic displacement parameters. All hydrogen atom positions were determined by geometry and refined by a riding model.

[Co(CH$_2$SiMe$_3$)(^{Cy}PNP)] (1). In a round-bottom flask, 200 mg (0.344 mmol) of [CoCl(^{Cy}PNP)] was dissolved in 10 mL of THF. To this solution was added dropwise 36 μL (0.36 mmol) of a 1.0 M solution of Me$_3$SiCH$_2$MgCl in THF. The reaction mixture was allowed to stir at room temperature for 30 min, during which time the color remained brown. The mixture was filtered through Celite, and all volatiles were removed in vacuo. The remaining residue was dissolved in toluene and filtered a second time through Celite to ensure removal of all Mg salts. The toluene solution was evaporated to dryness, producing a solid precipitate that was collected by filtration, washed with pentane, and dried in vacuo to afford 176 mg (80%) of a brown powder. Crystals suitable for X-ray diffraction were obtained from a concentrated 1,4-dioxane solution at 23 °C. ^{1}H NMR: δ 24.2 (4 H), 20.7 (4 H), 14.3 (4 H), 8.7 (4 H), 7.6 (4 H), 5.8 (4 H), 3.1 (4 H), 1.5 (8 H), 0.9 (4 H), −12.8 (9 *Me*$_3$Si), −41.9 (2 pyr-C*H*). Anal. Calcd for C$_{34}$H$_{61}$CoNP$_2$Si: C, 64.53; H, 9.72; N, 2.21. Found: C, 63.54; H, 9.58; N, 2.00.

[Co(H)(^{Cy}PNP)] (2). The species was observed in solution by treating [CoBr(^{Cy}PNP)] with 1 equiv of KHBEt$_3$ in THF or by exposure of degassed solutions of **1** and **3** to 1−2 bar of H$_2$. NMR: ^{1}H δ 46.8, 40.1, 22.3, 12.2, 9.3, 8.0, 4.1, −1.1, −1.4, −3.6, −38.5 (pyr-C*H*).

***cis*-[Co(H)$_2$(PMe$_3$)(^{Cy}PNP)] (4).** This species was observed in solution by treating **3** with 1−2 bar of H$_2$ in the presence of 1 equiv of PMe$_3$. NMR (toluene-d_8, 257 K): ^{1}H δ 6.44 (s, 2 pyr-C*H*), 3.15 (dt, 2 C*H*$_2$P), 2.90 (dt, 2 C*H*$_2$P), 2.32 (app d, 2 Cy), 1.99 (m, 4 Cy), 1.88−1.58 (20 Cy), 1.38 (m, 10 Cy), 1.16 (m, 8 Cy), 0.94 (app d, 9 P*Me*$_3$), −14.1 (br s, Co*H*), −21.6 (br s, Co*H*); ^{31}P{^{1}H} δ 89.0 (*P*Cy$_2$), 4.3 (*P*Me$_3$).

[Co(PMe$_3$)(^{Cy}PNP)] (5). A flask was charged with 150 mg (0.258 mmol) of **3** and 68 μL (2.5 equiv) of PMe$_3$. The mixture was dissolved in 10 mL of toluene, and the resulting purple solution was allowed to stir at room temperature for 12 h. The toluene was removed under reduced pressure to furnish 95 mg (88%) of a dark purple solid. Crystals suitable for X-ray diffraction were grown from a concentrated heptane solution of the complex at 23 °C. NMR: ^{1}H δ 6.55 (s, 2 pyr-C*H*), 2.96 (app t, 4 C*H*$_2$P), 2.33 (app d, 4 Cy), 1.82 (app t, 4 Cy), 1.77 (app d, 4 Cy), 1.72 (app d, 4 Cy), 1.62 (m, 8 Cy), 1.43 (m, 8 Cy), 1.27 (m, 8 Cy), 1.22 (m, 4 Cy) 1.11 (app t, 9 P*Me*$_3$); ^{31}P{^{1}H} δ 66.0 (*P*Cy$_2$), −1.1 (*P*Me$_3$). Anal. Calcd for C$_{33}$H$_{59}$CoNP$_3$: C, 63.76; H, 9.57; N, 2.25. Found: C, 60.03; H, 8.95; N, 1.93. Repeated analyses returned low values for C.

[Co(η^2-PhCCPh)(^{Cy}PNP)] (6). A round-bottom flask was charged with 100 mg (0.174 mmol) of **3** and 10 mL of toluene. To the brown solution was added 34 mg (0.19 mmol) of PhCCPh. The resulting solution was allowed to stir at ambient temperature for 12 h, during which time the color became more red. All volatiles were removed in vacuo to afford 98 mg (78%) of the crude product as a dark red powder. Further attempts to purify the material by recrystallization were unsuccessful. NMR: ^{1}H δ 8.30 (d, 4 *o*-Ph), 7.29 (t, 4 *m*-Ph), 7.13 (t, 2 *p*-Ph), 6.45 (s, 2 pyr-C*H*), 2.74 (app t, 4 C*H*$_2$P), 2.27 (app d, 4 Cy), 1.65 (app t, 4 Cy), 1.54 (app d, 12 Cy), 1.46 (app t, 8 Cy), 1.12 (app q, 4 Cy), 1.01 (app q, 4 Cy), 0.89 (m, 8 Cy); ^{13}C{^{1}H} δ 139.09 (t), 130.67, 130.21, 125.88, 105.25 (t), 88.20 (t), 33.87 (t), 29.98, 28.02, 27.82 (t), 27.55 (t), 26.71, 22.66 (t); ^{31}P{^{1}H} δ 46.70.

[Co(η^2-H$_2$CCHAr^{OMe})(^{Cy}PNP)] (7). In an NMR tube, compound **3** (10 mg, 17 μmol) was dissolved in 0.6 mL of benzene-d_6. To the solution was added 4.8 μL (36 μmol, 2 equiv) of 4-vinylanisole. The solution was then subjected to NMR analysis which displayed a 2:1 ratio of **7**:**3** along with free 4-vinylanisole. Small quantities of single crystalline material suitable for X-ray diffraction were obtained by slow cooling of a heptane solution of **3** in the presence of excess 4-vinylanisole at −30 °C. NMR: ^{1}H δ 7.68 (d, 2 *o*/*m*-Ph), 6.76 (d, 2 *o*/*m*-Ph), 6.41 (s, 2 pyr-C*H*), 3.86 (m, 1 vinyl-C*H*), 3.38 (s, 3 O*Me*), 2.8 (br s, 2 C*H*$_2$P), 2.6 (br s, 2 C*H*$_2$P), 2.50 (m, 1 vinyl-C*H*), 2.32 (app d, 2 Cy), 1.98 (m, 4 Cy), 1.8−1.0 (multiple overlapping Cy), 0.89 (m, 1 vinyl-C*H*); ^{31}P{^{1}H} 46.6 (AB pattern).

[Co(CCPh)(^{Cy}PNP)] (8). A flask was charged with 100 mg (0.17 mmol) of **3** and 10 mL of toluene. To the solution was added 20 μL (0.18 mmol) of phenylacetylene. The resulting mixture was allowed to stir at ambient temperature for 12 h. All volatiles were removed in vacuo, and the remaining solid was triturated with cold pentane and isolated by filtration to afford 87 mg (77%) of a red powder. Crystals suitable for X-ray diffraction were grown from a concentrated heptane solution at 23 °C. ^{1}H NMR: δ 40.6, 35.3, 21.2, 12.0, 9.5, 7.4, 7.1, 3.7, −0.3, −2.0, −8.3, −16.6, −45.8. Anal. Calcd for C$_{38}$H$_{55}$CoNP$_2$: C, 70.57; H, 8.57; N, 2.17. Found: C, 74.85; H, 9.15; N, 1.16. The high values for C and H and low values for N are consistent with retention of small quantities of heptane and toluene.

Hydrogenation Experiments. In the glovebox, a 50 mL Schlenk flask was charged with alkene or alkyne, 1,3,5-trimethylbenzene (internal standard), and compound **3** or **5** (0.5−2 mol %). The reactants were dissolved in 1 mL of benzene-d_6. The flask was sealed with a rubber septum and removed from the glovebox. A balloon containing ca. 2 bar of H$_2$ gas was fitted to the flask via a needle through the septum. The reaction was then permitted to stir at room temperature for the allotted time. Conversion of starting material and yield of product were assayed by NMR spectroscopy.

■ ASSOCIATED CONTENT

Supporting Information

The Supporting Information is available free of charge at https://pubs.acs.org/doi/10.1021/acs.organomet.1c00053.

NMR spectra, additional structural diagrams, and tables of crystallographic data and refinement parameters (PDF)

Accession Codes

CCDC 2059458−2059461 contain the supplementary crystallographic data for this paper. These data can be obtained free of charge via www.ccdc.cam.ac.uk/data_request/cif, or by emailing data_request@ccdc.cam.ac.uk, or by contacting The Cambridge Crystallographic Data Centre, 12 Union Road, Cambridge CB2 1EZ, UK; fax: +44 1223 336033.

https://dx.doi.org/10.1021/acs.organomet.1c00053
Organometallics XXXX, XXX, XXX−XXX

AUTHOR INFORMATION

Corresponding Author

Zachary J. Tonzetich − *Department of Chemistry, University of Texas at San Antonio (UTSA), San Antonio, Texas 78249, United States;* orcid.org/0000-0001-7010-8007; Email: zachary.tonzetich@utsa.edu

Authors

Hussah Alawisi − *Department of Chemistry, University of Texas at San Antonio (UTSA), San Antonio, Texas 78249, United States; Department of Chemistry, King Faisal University, Al Hofuf, Kingdom of Saudi Arabia*

Hadi D. Arman − *Department of Chemistry, University of Texas at San Antonio (UTSA), San Antonio, Texas 78249, United States*

Complete contact information is available at: https://pubs.acs.org/10.1021/acs.organomet.1c00053

Notes

The authors declare no competing financial interest.

ACKNOWLEDGMENTS

The authors thank the Welch Foundation (AX-1772) for financial support of this work. NMR and X-ray crystallographic facilities at UTSA are supported by grants from the National Science Foundation (CHE-1625963 and CHE-1920057).

REFERENCES

(1) Chirik, P. J. Modern Alchemy: Replacing Precious Metals with Iron in Catalytic Alkene and Carbonyl Hydrogenation Reactions. *Catalysis without Precious Metals* **2010**, 83−110.

(2) Morris, R. H. Exploiting Metal-Ligand Bifunctional Reactions in the Design of Iron Asymmetric Hydrogenation Catalysts. *Acc. Chem. Res.* **2015**, *48*, 1494−1502.

(3) Chirik, P. J. Iron- and Cobalt-Catalyzed Alkene Hydrogenation: Catalysis with Both Redox-Active and Strong Field Ligands. *Acc. Chem. Res.* **2015**, *48*, 1687−1695.

(4) Robinson, S. J. C.; Heinekey, D. M. Hydride & dihydrogen complexes of earth abundant metals: structure, reactivity, and applications to catalysis. *Chem. Commun.* **2017**, *53*, 669−676.

(5) Liu, W.; Sahoo, B.; Junge, K.; Beller, M. Cobalt Complexes as an Emerging Class of Catalysts for Homogeneous Hydrogenations. *Acc. Chem. Res.* **2018**, *51*, 1858−1869.

(6) Kallmeier, F.; Kempe, R. Manganese Complexes for (De)-Hydrogenation Catalysis: A Comparison to Cobalt and Iron Catalysts. *Angew. Chem., Int. Ed.* **2018**, *57*, 46−60.

(7) Seo, C. S. G.; Morris, R. H. Catalytic Homogeneous Asymmetric Hydrogenation: Successes and Opportunities. *Organometallics* **2019**, *38*, 47−65.

(8) Ai, W.; Zhong, R.; Liu, X.; Liu, Q. Hydride Transfer Reactions Catalyzed by Cobalt Complexes. *Chem. Rev.* **2019**, *119*, 2876−2953.

(9) Filonenko, G. A.; van Putten, R.; Hensen, E. J. M.; Pidko, E. A. Catalytic (de)hydrogenation promoted by non-precious metals − Co, Fe and Mn: recent advances in an emerging field. *Chem. Soc. Rev.* **2018**, *47*, 1459−1483.

(10) Peris, E.; Crabtree, R. H. Key factors in pincer ligand design. *Chem. Soc. Rev.* **2018**, *47*, 1959−1968.

(11) Merz, L. S.; Ballmann, J.; Gade, L. H. Phosphines and N-Heterocycles Joining Forces: an Emerging Structural Motif in PNP-Pincer Chemistry. *Eur. J. Inorg. Chem.* **2020**, *2020*, 2023−2042.

(12) Wei, Z.; Jiao, H. Bifunctional aliphatic PNP pincer catalysts for hydrogenation: Mechanisms and scope. *Adv. Inorg. Chem.* **2019**, *73*, 323−384.

(13) Ganguly, G.; Malakar, T.; Paul, A. Theoretical Studies on the Mechanism of Homogeneous Catalytic Olefin Hydrogenation and Amine−Borane Dehydrogenation by a Versatile Boryl-Ligand-Based Cobalt Catalyst. *ACS Catal.* **2015**, *5*, 2754−2769.

(14) Zhang, G.; Vasudevan, K. V.; Scott, B. L.; Hanson, S. K. Understanding the mechanisms of cobalt-catalyzed hydrogenation and dehydrogenation reactions. *J. Am. Chem. Soc.* **2013**, *135*, 8668−8681.

(15) Gorgas, N.; Brünig, J.; Stöger, B.; Vanicek, S.; Tilset, M.; Veiros, L. F.; Kirchner, K. Efficient Z-Selective Semihydrogenation of Internal Alkynes Catalyzed by Cationic Iron(II) Hydride Complexes. *J. Am. Chem. Soc.* **2019**, *141*, 17452−17458.

(16) Wang, Y.; Zhu, L.; Shao, Z.; Li, G.; Lan, Y.; Liu, Q. Unmasking the Ligand Effect in Manganese-Catalyzed Hydrogenation: Mechanistic Insight and Catalytic Application. *J. Am. Chem. Soc.* **2019**, *141*, 17337−17349.

(17) Ritz, M. D.; Parsons, A. M.; Palermo, P. N.; Jones, W. D. Bisoxazoline-pincer ligated cobalt-catalyzed hydrogenation of alkenes. *Polyhedron* **2020**, *180*, 114416.

(18) Zuo, Z.; Xu, S.; Zhang, L.; Gan, L.; Fang, H.; Liu, G.; Huang, Z. Cobalt-Catalyzed Asymmetric Hydrogenation of Vinylsilanes with a Phosphine-Pyridine-Oxazoline Ligand: Synthesis of Optically Active Organosilanes and Silacycles. *Organometallics* **2019**, *38*, 3906−3911.

(19) Muhammad, S. R.; Nugent, J. W.; Tokmic, K.; Zhu, L.; Mahmoud, J.; Fout, A. R. Electronic Ligand Modifications on Cobalt Complexes and Their Application toward the Semi-Hydrogenation of Alkynes and Para-Hydrogenation of Alkenes. *Organometallics* **2019**, *38*, 3132−3138.

(20) Merz, L. S.; Blasius, C. K.; Wadepohl, H.; Gade, L. H. Square Planar Cobalt(II) Hydride versus T-Shaped Cobalt(I): Structural Characterization and Dihydrogen Activation with PNP-Cobalt Pincer Complexes. *Inorg. Chem.* **2019**, *58*, 6102−6113.

(21) Landge, V. G.; Pitchaimani, J.; Midya, S. P.; Subaramanian, M.; Madhu, V.; Balaraman, E. Phosphine-free cobalt pincer complex catalyzed Z-selective semi-hydrogenation of unbiased alkynes. *Catal. Sci. Technol.* **2018**, *8*, 428−433.

(22) Brzozowska, A.; Azofra, L. M.; Zubar, V.; Atodiresei, I.; Cavallo, L.; Rueping, M.; El-Sepelgy, O. Highly Chemo- and Stereoselective Transfer Semihydrogenation of Alkynes Catalyzed by a Stable, Well-Defined Manganese(II) Complex. *ACS Catal.* **2018**, *8*, 4103−4109.

(23) Tokmic, K.; Markus, C. R.; Zhu, L.; Fout, A. R. Well-Defined Cobalt(I) Dihydrogen Catalyst: Experimental Evidence for a Co(I)/Co(III) Redox Process in Olefin Hydrogenation. *J. Am. Chem. Soc.* **2016**, *138*, 11907−11913.

(24) Tokmic, K.; Fout, A. R. Alkyne Semihydrogenation with a Well-Defined Nonclassical Co−H_2 Catalyst: A H_2 Spin on Isomerization and E-Selectivity. *J. Am. Chem. Soc.* **2016**, *138*, 13700−13705.

(25) Fu, S.; Chen, N.-Y.; Liu, X.; Shao, Z.; Luo, S.-P.; Liu, Q. Ligand-Controlled Cobalt-Catalyzed Transfer Hydrogenation of Alkynes: Stereodivergent Synthesis of Z- and E-Alkenes. *J. Am. Chem. Soc.* **2016**, *138*, 8588−8594.

(26) Chen, J.; Chen, C.; Ji, C.; Lu, Z. Cobalt-Catalyzed Asymmetric Hydrogenation of 1,1-Diarylethenes. *Org. Lett.* **2016**, *18*, 1594−1597.

(27) Lin, T.-P.; Peters, J. C. Boryl-Mediated Reversible H2 Activation at Cobalt: Catalytic Hydrogenation, Dehydrogenation, and Transfer Hydrogenation. *J. Am. Chem. Soc.* **2013**, *135*, 15310−15313.

(28) Zhang, G.; Scott, B. L.; Hanson, S. K. Mild and homogeneous cobalt-catalyzed hydrogenation of C:C, C:O, and C:N bonds. *Angew. Chem., Int. Ed.* **2012**, *51*, 12102−12106.

(29) Monfette, S.; Turner, Z. R.; Semproni, S. P.; Chirik, P. J. Enantiopure C1-Symmetric Bis(imino)pyridine Cobalt Complexes for Asymmetric Alkene Hydrogenation. *J. Am. Chem. Soc.* **2012**, *134*, 4561−4564.

(30) Junge, K.; Papa, V.; Beller, M. Cobalt-Pincer Complexes in Catalysis. *Chem. - Eur. J.* **2019**, *25*, 122−143.

(31) Liu, X.; Liu, B.; Liu, Q. Migratory Hydrogenation of Terminal Alkynes by Base/Cobalt Relay Catalysis. *Angew. Chem., Int. Ed.* **2020**, *59*, 6750−6755.

(32) Bullock, R. M. A Mercurial Route to a Cobalt Dihydrogen Complex. *Angew. Chem., Int. Ed.* **2011**, *50*, 4050−4052.

(33) Knijnenburg, Q.; Horton, A. D.; Heijden, H. v. d.; Kooistra, T. M.; Hetterscheid, D. G. H.; Smits, J. M. M.; Bruin, B. d.; Budzelaar, P. H. M.; Gal, A. W. Olefin hydrogenation using diimine pyridine complexes of Co and Rh. *J. Mol. Catal. A: Chem.* **2005**, *232*, 151−159.
(34) Thompson, C. V.; Tonzetich, Z. J. Pincer ligands incorporating pyrrolyl units: Versatile platforms for organometallic chemistry and catalysis. *Adv. Organomet. Chem.* **2020**, *74*, 153−240.
(35) Alawisi, H.; Al-Afyouni, K. F.; Arman, H. D.; Tonzetich, Z. J. Aldehyde Decarbonylation by a Cobalt(I) Pincer Complex. *Organometallics* **2018**, *37*, 4128−4135.
(36) Krishnan, V. M.; Arman, H. D.; Tonzetich, Z. J. Preparation and reactivity of a square-planar PNP cobalt(II)−hydrido complex: isolation of the first $\{Co-NO\}^8$−hydride. *Dalton Trans.* **2018**, *47*, 1435−1441.
(37) Kuriyama, S.; Arashiba, K.; Tanaka, H.; Matsuo, Y.; Nakajima, K.; Yoshizawa, K.; Nishibayashi, Y. Direct Transformation of Molecular Dinitrogen into Ammonia Catalyzed by Cobalt Dinitrogen Complexes Bearing Anionic PNP Pincer Ligands. *Angew. Chem., Int. Ed.* **2016**, *55*, 14291−14295.
(38) Rummelt, S. M.; Zhong, H.; Léonard, N. G.; Semproni, S. P.; Chirik, P. J. Oxidative Addition of Dihydrogen, Boron Compounds, and Aryl Halides to a Cobalt(I) Cation Supported by a Strong-Field Pincer Ligand. *Organometallics* **2019**, *38*, 1081−1090.
(39) Qi, X.; Liu, X.; Qu, L.-B.; Liu, Q.; Lan, Y. Mechanistic insight into cobalt-catalyzed stereodivergent semihydrogenation of alkynes: The story of selectivity control. *J. Catal.* **2018**, *362*, 25−34.
(40) *CrystalClear User's Manual*; Rigaku Corporation: The Woodlands, TX, 2011.
(41) *CrysAlisPro*; Rigaku Oxford Diffraction: Rigaku Corporation: The Woodlands, TX, 2015.
(42) *SCALE3 ABSPACK: An Oxford Diffraction Program*; Oxford Diffraction Ltd.: Abingdon, Oxfordshire, U.K., 2005.
(43) Dolomanov, O. V.; Bourhis, L. J.; Gildea, R. J.; Howard, J. A. K.; Puschmann, H. OLEX2: a complete structure solution, refinement and analysis program. *J. Appl. Crystallogr.* **2009**, *42*, 339−341.
(44) Sheldrick, G. M. *SHELXTL97: Program for Refinement of Crystal Structures*; University of Göttingen: Göttingen, Germany, 1997.
(45) Sheldrick, G. M. A short history of SHELX. *Acta Crystallogr., Sect. A: Found. Crystallogr.* **2008**, *A64*, 112−122.

https://dx.doi.org/10.1021/acs.organomet.1c00053
Organometallics XXXX, XXX, XXX−XXX